Passivation of Silicon Surface by Laser Rapid Heating

H. Abe[1], C. Akiyama[1], M. Hasumi[1], T. Sameshima[1], T. Mizuno[2], and N. Sano[3]
[1] Tokyo University of Agriculture and Technology, 2-24-16, Naka-cho, Koganei, 184-8588, Japan
E-mail: tsamesim@cc.tuat.ac.jp
[2] Kanagawa University, 2946 Tsuchiya, Hiratsuka 259-1293, Japan
[3] Aurea Works Corporation, 75-1, Ono-cho, Tsurumi-ku, Yokohama 230-0046, Japan

We report rapid laser-induced passivation of the silicon surface. When the top surfaces of n-type 500-μm-thick silicon substrates with surfaces coated with 100 nm thermally grown SiO_2 layers (initial samples) were irradiated with Ar plasma at 50 W for 120 s, the 635-nm-light induced minority carrier effective lifetime τ_{eff} decreased from $1.7x10^{-3}$ (initial) to $1.7x10^{-5}$ s because Ar plasma caused substantial carrier recombination defect states at the silicon surfaces. τ_{eff} was markedly increased to $1.7x10^{-3}$ s by 940-nm-semiconductor laser irradiation at $3.57x10^4$ W/cm^2 for 4 ms. Laser heating effectively decreased the density of plasma induced carrier recombination defect. However, laser heating of the initial sample at $4.0x10^4$ W/cm^2 decreased τ_{eff} from $2.2x10^{-3}$ (initial) to $1.7x10^{-4}$ s. Additional laser heating at $3.70x10^4$ W/cm^2 increased τ_{eff} to $3.9x10^{-4}$ s-and it partially cured laser induced carrier recombination defects.

DOI: 10.2961/jlmn.2014.02.0012

Keywords: minority carrier effective lifetime, laser heating, semiconductor laser, microwave absorption, carrier recombination

1. Introduction

Laser heating is an attractive method for activating silicon semiconductor implanted with dopant atoms [1-6]. A high activation ratio and no marked impurity diffusion are achieved by laser-induced rapid heating. No substrate heating is necessary because laser heating energy effectively concentrates in the surface region during short irradiation time. It is important to reduce the thermal budget for fabricating semiconductor devices at a low cost. A laser heating is also attractive for annealing of semiconductor surface region. Defects located at the surface region will be reduced and thermally stable state will be achieved by laser heating with no substrate heating. However, we recently found that laser heating decreased the minority carrier effective lifetime τ_{eff} of silicon substrate [7]. Decrease in τ_{eff} will be a serious problem for application of laser heating to fabrication of high efficiency solar cells and high sensitivity photo sensors because of low light sensitivity.

In this paper, we discuss laser-induced passivation of silicon surface by 940-nm semiconductor laser heating. We demonstrate that laser heating effectively increases τ_{eff}, which was beforehand decreased by Ar plasma irradiation. The laser power condition for increase in τ_{eff} is limited. We also demonstrate decrease in τ_{eff} by laser irradiation at a high power intensity. We discuss physics of laser heating to annihilate or create carrier recombination defects.

2. Experimental

12 Ωcm n-type 500-μm-thick silicon substrates were prepared. The top and rear surfaces were coated with 100-nm-thick thermally grown SiO_2 layers formed in 1100°C wet oxygen atmosphere. The silicon samples were irradiated with 940-nm infrared semiconductor laser. Figure 1 shows a schematic apparatus of laser heating. The laser beam with a maximum power of 25 W was introduced using an optical fiber. The optical fiber and optics with a lens were mounted on an *X-Y* mobile stage. The laser beam was focused by the lens to a spot with a Gaussian intensity distribution and a diameter of 200 μm at full width and maximum half at the sample surface. Samples were placed on a 1-mm-thick quartz glass plate in a direction normal to the laser beam. The laser beam was moved in the *Y*-direction at 5 cm/s at power intensities ranging from $2.67x10^4$ to $4.46x10^4$ W/cm^2 at sample surface. Irradiation duration was 4ms. The laser beam was stepwise moved in the *X*-direction at a step of 100 μm. The top surface of the sample with an area of 4 x 5 cm^2 was completely heated by laser irradiation with a overlapping ratio of 50% for 4ms. Heat flow calculation using a numerical finite-element program resulted in heating to 1060 K at the top surface for conditions of a laser intensity of $4.46x10^4$ W/cm^2 and a light reflection loss of 17 % at 940 nm.

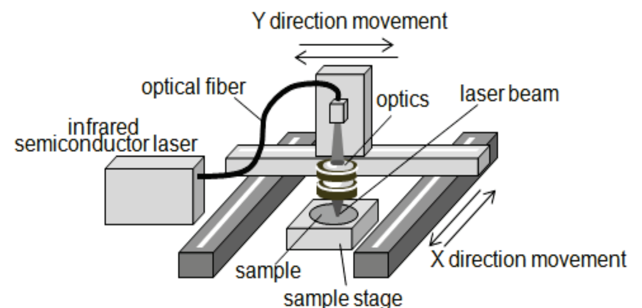

Fig. 1. Schematic apparatus of infrared semiconductor laser heating.

The top surfaces of the samples were irradiated by 13.56 MHz radio-frequency (RF)-capacitance-coupled Ar plasma at 50 W and 1.0 Pa for 120 s [8]. A sample was placed on a metal plate electrically grounded in a chamber facing a metal electrode applied at RF voltage. Ar gas was introduced at 50sccm under evacuation using a turbo-molecular pump.

Figure 2 shows a schematic of the 9.35 GHz microwave transmittance measurement system with waveguide tubes, which had a narrow gap for placing a sample wafer. Continuous wave (CW) 635 nm laser diode (LD) lights at 1.5 mW/cm^2 were introduced in the waveguide tube, as shown in Fig. 2. The microwave which transmitted samples was rectified using a high-speed diode and analyzed to obtain τ_{eff} [9,10]. We constructed a finite-element numerical calculation program including theories of carrier generation associated with optical absorption coefficients, carrier diffusion, and annihilation to estimate the carrier recombination defect states from experimental τ_{eff} (top) and τ_{eff} (rear) obtained by light illumination to the top and rear surfaces, respectively [11,12].

After the microwave transmittance measurement, the SiO_2 layers at the rear surface were removed by 5% hydrofluoric acid. Al metal electrodes were formed at the top and rear surfaces by the vacuum evaporation. The capacitance response at 1 MHz alternative voltage with an amplitude of 10 mV as a function of the bias voltage (C-V) was measured.

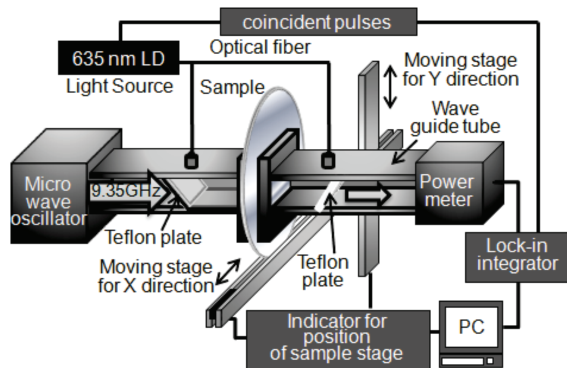

Fig. 2. Schematic apparatus of the 9.35 GHz microwave transmittance measurement system

3. Results and discussion

Figures 3 shows τ_{eff} (top) (open circles) and τ_{eff} (rear) (solid circles) as a function of laser power intensity for laser irradiation applied to the initial (a) and Ar plasma irradiated samples (b). τ_{eff} (top) and τ_{eff} (rear) had a high value of $1.5x10^{-3}$ s for the initial sample, as shown by the arrow in Fig. 3(a). This means that the initial sample had a high quality crystalline bulk and the surfaces well passivated with thermally grown SiO_2 layers. The samples were irradiated with 940-nm-laser light with stepwise increasing its power intensity. τ_{eff} (top) and τ_{eff} (rear) were decreased by irradiation above $4.00x10^4$ W/cm^2. They decreased to $2.5x10^{-6}$ and $1.4x10^{-4}$ s at $4.46x10^4$ W/cm^2 as shown in Fig.

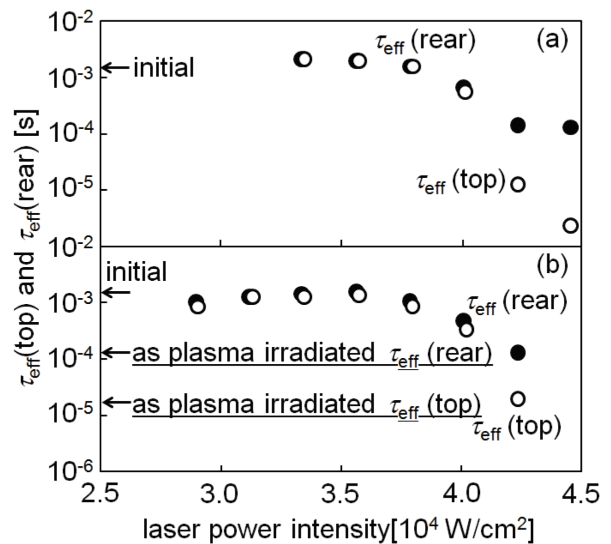

Fig. 3. τ_{eff} (top) (open circles) and τ_{eff} (rear) (solid circles) as a function of laser power intensity for laser irradiation applied to the initial (a) and Ar plasma irradiated samples (b).

3 (a). Those results mean that a high density of carrier recombination defect sites was generated at the surface region by infrared laser heating with a high power. The defect sites caused by laser irradiation effectively annihilate photo-induced carriers generated by 635-nm-light illuminations to the top surface. τ_{eff} (top) was therefore very low. In contrast, photo-induced carriers generated by 635-nm-light illumination to the rear surface traveled across the 500-µm-thick substrate from the rear to the top surfaces and then they were annihilated by the recombination defect sites. Therefore, they were alive long during diffusion in the substrate and τ_{eff} (rear) was high [7].

When Ar plasma was applied to the initial sample, τ_{eff} (top) and τ_{eff} (rear) decreased from the initial value of $1.7x10^{-3}$ s to $1.7x10^{-5}$ and $1.4x10^{-4}$ s, as shown by three arrows in Fig. 3(b). The plasma irradiated sample was heated by laser with stepwise increasing its power intensity. τ_{eff} (top) and τ_{eff} (rear) increased to $1.7x10^{-3}$ s, almost the same as that of the initial sample, as the laser power intensity increased from $2.67x10^4$ up to $3.57x10^4$ W/cm^2. Laser heating cured the defect states caused by the Ar plasma irradiation. However, τ_{eff} (top) and τ_{eff} (rear) were decreased again by laser irradiation above $4.0x10^4$ W/cm^2 for the plasma irradiated sample similar to the case of the initial sample. The results of Fig. 3 show that laser heating plays different roles of defect reduction and defect generation, which depended on the laser power intensity.

We then prepared the samples by two-step 940-nm-laser irradiation. For the first time, the initial samples were heated with 940-nm-laser light at $4.00x10^4$ and $4.40x10^4$ W/cm^2. Then the samples were irradiated again by 940-nm-laser light with stepwise increasing the power intensity. Figure 4 shows τ_{eff} (top) (open circles and squares) and τ_{eff} (rear) (solid circles and squares) as a function of laser power intensity at second irradiation. The first laser irradiation at $4.00x10^4$ W/cm^2 decreased τ_{eff} (top) and τ_{eff} (rear)

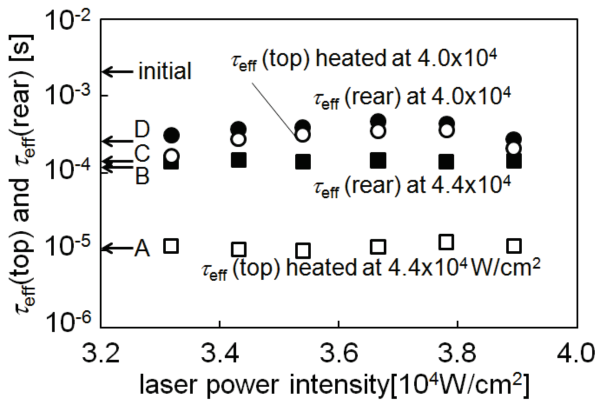

Fig. 4. τ_{eff} (top) (open marks) and τ_{eff} (rear) (solid marks) as a function of laser power intensity at second irradiation. Arrows A and B present τ_{eff} (top) and τ_{eff} (rear), for sample laser irradiated at $4.4x10^4$ W/cm^2. Arrows C and D present τ_{eff} (top) and τ_{eff} (rear), for sample laser irradiated at $4.0x10^4$ W/cm^2.

of $1.7x10^{-4}$ and $2.9x10^{-4}$ s, as shown by arrows C and D in Fig. 4. They were increased to $3.9x10^{-4}$ and $5.2x10^{-4}$ s by second laser irradiation up to $3.70x10^4$ W/cm^2. This indicates that the density of carrier recombination defect states was decreased by second laser irradiation. On the other hand, when the samples were irradiated with laser at $4.40x10^4$ W/cm^2, τ_{eff} (top) and τ_{eff} (rear) were decreased to $1.1x10^{-5}$ and $1.5x10^{-4}$ s, as shown by arrows A and B, respectively, as shown in Fig. 4. They were hardly changed by second laser irradiation between $3.30x10^4$ and $3.90x10^4$ W/cm^2. Defect states formed by high power laser irradiation were not cured by second laser irradiation.

Figure 5 shows C-V characteristics for the initial sample, laser irradiated samples at $4.00x10^4$, and $4.40x10^4$ W/cm^2, and two step laser irradiated samples at $4.0x10^4$ followed by $3.70x10^4$ W/cm^2, and at $4.40x10^4$ W/cm^2 followed by $3.70x10^4$ W/cm^2 (a) and the plasma irradiated sample and sample plasma irradiated followed by laser irradiated at $3.57x10^4$ W/cm^2 (b). Sharp change in capacitance was observed for the initial sample. It means that the sample had a low density of interface traps. Capacitance change became gentle in the cases of laser irradiation at $4.0x10^4$ and $4.4x10^4$ W/cm^2 because of generation of interface trap states. Capacitance change became sharp in the case of two step laser irradiation at $4.0x10^4$ followed by $3.7x10^4$ W/cm^2, while the change in capacitance kept gentle in the case of laser irradiation at $4.4x10^4$ followed by $3.7x10^4$ W/cm^2, as shown in Fig. 5(a). Ar plasma treatment made capacitance change very gentle. Ar plasma irradiation caused substantial interface traps. Subsequent laser irradiation at $3.57x10^4$ W/cm^2 made capacitance change sharp similar to that of the initial sample.

The density of surface carrier recombination defect states D_r and the density of interface traps D_{it} at the mid gap were estimated from experimental τ_{eff} (top) and τ_{eff} (rear), and C-V characteristics, as shown in Figs. 3-5 [13]. Figure 6 shows D_r (a) and D_{it} (b) for samples shown by their C-V curves in Fig. 5. D_r and D_{it} were low of $7.6x10^9$ cm^{-2} and $5.9x10^9$ cm^{-2}eV^{-1} for the initial sample. They increased to $3.1x10^{12}$ cm^{-2} and $3.8x10^{11}$ cm^{-2}eV^{-1} for the

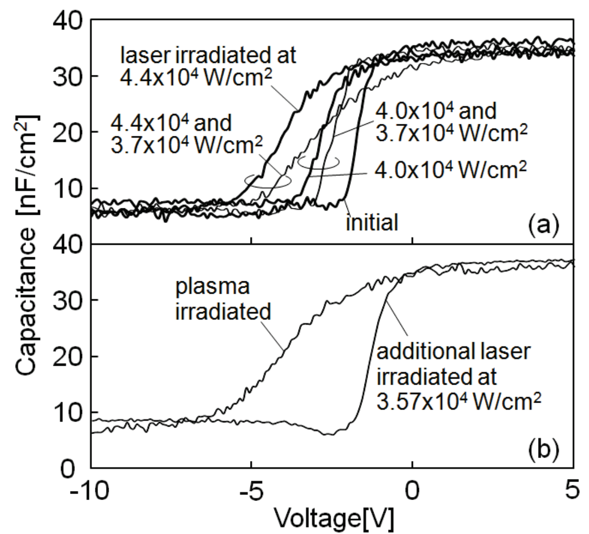

Fig. 5. C-V characteristics for the initial sample, laser irradiated samples at $4.0x10^4$ and $4.4x10^4$ W/cm^2, and two step laser irradiated samples at $4.0x10^4$ followed by $3.7x10^4$ W/cm^2, and at $4.4x10^4$ followed by $3.7x10^4$ W/cm^2 (a) and the plasma irradiated sample and sample plasma irradiated followed by laser irradiated at $3.57x10^4$ W/cm^2 (b).

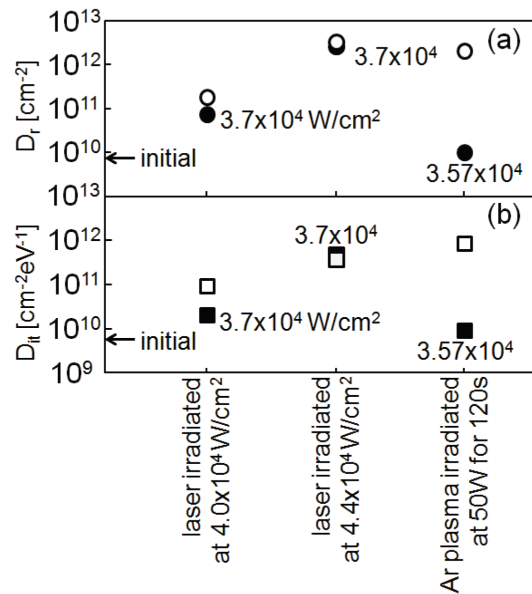

Fig. 6. D_r (a) and D_{it} (b) for samples shown in Fig. 5. Open marks present D_r and D_{it} for first laser or plasma treatment. Solid marks present D_r and D_{it} for second laser treatment. Power intensities at second laser irradiation present in the figure.

$4.40x10^4$ W/cm^2 laser irradiated sample. The high power laser heating made D_r much higher than D_{it}. This indicates that high power laser induced defects are very sensitive to carrier recombination. In the case of laser irradiation $4.00x10^4$ W/cm^2 D_r and D_{it} were $1.8x10^{11}$ cm^{-2} and $8.4x10^{10}$ cm^{-2}eV^{-1}. Low D_r and D_{it} were obtained to be $6.9x10^{10}$ cm^{-2} and $1.8x10^{10}$ cm^{-2}eV^{-1} by two step laser irradiation at $4.0x10^4$ followed by $3.70x10^4$ W/cm^2, although they were kept high as $2.9x10^{12}$ cm^{-2} and $4.2x10^{11}$ cm^{-2}eV^{-1} by two step laser irradiation at $4.40x10^4$ followed by

$3.70x10^4$ W/cm^2. D_r and D_{it} were increased to $1.9x10^{12}$ cm^{-2} and $7.9x10^{11}$ cm^{-2}eV^{-1} by the plasma irradiation. Plasma induced defects were sensitive to carrier trap as well as carrier recombination. D_r and D_{it} decreased to $8.8x10^9$ cm^{-2} and $8.1x10^9$ cm^{-2}eV^{-1} by additional laser irradiation at $3.57x10^4$ W/cm^2. Defect states caused by plasma irradiation were easily eliminated by laser irradiation, in contrast to the case of defect states caused by high power laser irradiation $4.40x10^4$ W/cm^2, which were hardly cured by additional laser heating.

Via those experimental results and analyses, we interpret that the point defects such as lattice vacancies (point defects) are mainly generated in the case of plasma irradiation and laser rapid heating at a low power. The point defects play roles in carrier recombination and carrier trap. They are easily eliminated by subsequent laser heating because interstitial silicon atoms are moved back to the lattice sites by laser heating. When samples were heated with high power intensity at $4.40x10^4$ W/cm^2, large scale defects such as dislocation loops or vacancy clusters were probably formed [14]. Many silicon atoms moved and this mass action probably forms the large scaled defects. Those defects would not be removed by additional laser heating. Crystallographic analysis is further necessary to make defect structure formed by high power laser irradiation clear.

4. Summary

We investigated laser-induced passivation silicon surface using 940-nm semiconductor laser heating. 12 Ωcm n-type 500-μm-thick silicon substrates coated with 100-nm-thick thermally grown SiO_2 layers were prepared. τ_{eff} (top) and τ_{eff} (rear) were decreased to $2.5x10^{-6}$ and $1.4x10^{-4}$ s by laser irradiation up to $4.46x10^4$ W/cm^2 for 4ms. They were also decreased to $1.7x10^{-5}$ and $1.4x10^{-4}$ s by 13.56 MHz RF Ar plasma at 50 W and 1.0 Pa for 120 s. The substantial carrier recombination defect states were formed by high power laser and Ar plasma irradiation.

Additional laser heating was carried out for investigating increase in τ_{eff}. For the Ar plasma irradiated sample, τ_{eff} (top) and τ_{eff} (rear) were increased to $1.7x10^{-3}$ s, which was almost the same level of the initial sample by laser irradiation at $3.57x10^4$ W/cm^2. In the case of laser irradiation at $4.00x10^4$ W/cm^2, τ_{eff} (top) and τ_{eff} (rear) were decreased to $1.7x10^{-4}$ and $2.9x10^{-4}$ s. They were increased to $3.9x10^{-4}$ and $5.2x10^{-4}$ s by additional laser irradiation at $3.7x10^4$ W/cm^2. Change in τ_{eff} was similar to the case of Ar plasma irradiation. However, when the initial sample was heated by laser at $4.40x10^4$ W/cm^2, τ_{eff} (top) and τ_{eff} (rear) decreased to $1.1x10^{-5}$ and $1.5x10^{-4}$ s. They were hardly changed by additional laser irradiation at $3.70x10^4$ W/cm^2. Analysis of C-V characteristics gave decrease in D_{it} to $8.1x10^9$ cm^{-2}eV^{-1} in the case of laser heating of Ar plasma irradiated sample. Although D_{it} was decreased to $1.8x10^{10}$ cm^{-2}eV^{-1} by second laser irradiation at $3.7x10^4$ W/cm^2 of the sample first heated by laser irradiation at $4.00x10^4$ W/cm^2, it kept a high value of $4.2x10^{11}$ cm^{-2}eV^{-1} in the case of second laser heating at $4.00x10^4$ W/cm^2 of the sample first heated at $4.40x10^4$ W/cm^2. Experimental results shows that laser heating is effective to decrease the densities of carrier recombination states and carrier traps caused by Ar plasma irradiation and laser heating at a low power of $4.00x10^4$ W/cm^2. We interpret that lattice vacancies were generated by those processes, and that they are effectively eliminated by additional laser heating. On the other hand, additional laser heating did not decrease the density of defects caused by laser heating at a higher intensity of $4.40x10^4$ W/cm^2. Defects were probably too large for rapid laser heating to eliminate them.

Acknowledgments

This work was partly supported by Grant-in-Aid for Science Research C (No. 25420282 and 23560360) from the Ministry of Education, Culture, Sports, Science and Technology of Japan, and Sameken Co., Ltd.

References

[1] E. I. Shtyrkov, I. B. Khaibullin, M. M. Zaripov, M. F. Galyatudinov, and R. M. Bayasitov: Sov. Phys. –Semicond. (enbl. Transl.) 9 (1975) 1309.

[2] D. H. Lowndes, G. H. Kirkpatrick, Jr., S. J. Pennycook, S. P. Withrow, and D. N. Mashburn: Appl. Phys. Lett. 48 (1986) 1389.

[3] T. F. Deutsch, J. C. C. Fan, C. W. Turner, R. L. Chapman, D. J. Ehrlich and R. M. Osgood, Jr.: Appl. Phys. Lett., 38 (1981) 144.

[4] T. Sameshima, S. Usui, and M. Sekiya: J. Appl. Phys. 62 (1987) 711.

[5] T. Sameshima, M. Maki, M. Takiuchi, N. Andoh, N. Sano, Y. Matsuda, and Y. Andoh: Jpn. J. Appl. Phys. 46 (2007) 6474.

[6] K. Ukawa, Y. Kanda, T. Sameshima, N. Sano, M. Naito, and N. Hamamoto: Jpn. J. Appl. Phys. 49 (2010) 076503.

[7] T. Sameshima, K. Betsuin, T. Mizuno and N. Sano: Jpn. J. Appl. Phys. 51 (2012)03CA04-1-6.

[8] M. Hasumi, J. Takenezawa, T. Nagao, and T. Sameshima: Jpn. J. Appl. Phys 50 (2011)03CA03-1-4.

[9] T. Sameshima, H. Hayasaka, and T. Haba: Jpn. J.Appl. Phys. 48 (2009) 021204-1.

[10]T. Sameshima, T. Nagao, S. Yoshidomi, K. Kogure, and M. Hasumi: Jpn. J. Appl. Phys 50 (2011)03CA02.

[11] A. S. Groove: Physics and Technology of Semiconductor Devices (Wiley, New York, 1967) Chap. 5.

[12] D. J. Fitgerald and A. S. Grove: Proc. IEEE, 54 (1966) 1601.

[13] Y. Taur and T. Ning: *Fundamental of Modern VLSI Physics* (Cambridge University Press, Cambridge ,U. K. 1998) Chap. 2.

[14] S. S. Kapur, *Dissertation of University of Pennsylvanisa,* (Publicly accessible Penn Dissertations, 2010).109.

(Received: July 22, 2013, Accepted: April 19, 2014)